Investigation of Coupled Lateral and Torsional Vibrations of a Cracked Rotor Under Radial Load

Xi Wu, Assistant Professor
Jim Meagher, Professor
Clinton Judd, Graduate Student

Department of Mechanical Engineering
California Polytechnic State University, San Luis Obispo, CA93407-0358

NOMENCLATURE

$\omega_n,\ \omega_t$	lateral and torsional natural frequencies, respectively.
Θ	angular displacement of inboard disk.
θ	angular rotation of the inboard disk relative to motor.
θ_0	initial angular location of inboard disk.
Φ	angular rotation of outboard disk.
φ	angular rotation of the outboard disk relative to motor.
φ_0	initial angular location of outboard disk.
I_0	inboard disk polar moment of inertia.
I	outboard disk polar moment of inertia.
δ	angular orientation of outboard disk eccentricity.
Γ_c	lateral coupling terms in outboard disk equation of motion.
M	outboard disk mass.
P	vertical side load.
X,Y	outboard disk lateral motion in inertial coordinates.
ξ,η	rotor fixed rotating coordinates.
Y_m	dynamic vertical vibration in inertial coordinates.
ε	eccentricity of outboard disk.
C_c, K_c	motor-shaft coupling damping and stiffness, respectively.
$C,\ C_t$	lateral and torsional damping coefficients, respectively.
$\zeta,\ \zeta_t$	lateral and torsional damping ratios, respectively.
Ω	motor speed.
K_t	torsional shaft stiffness.
K	uncracked shaft lateral stiffness.
$f(\Phi)$	crack steering function.
ρ :	radius of gyration.
$\Delta k_\xi,\ \Delta k_\eta$	the reduced stiffness in ξ and η directions, respectively.

ABSTRACT

A practical cracked rotor model with two disks representing a turbine and generator is studied using a four degree of freedom model; two transverse displacements and two torsional angular displacements. The differential equations of a rotor with a crack, unbalance, and constant radial force are first derived in detail using energy principles. The nonlinearities related with a “breathing” crack are incorporated, which distinguishes this paper from others studying stiffness anisotropy of a rotor with a similar rotor configuration. Through numerical simulations, this paper demonstrates the lateral-torsional coupling that occurs with a shaft crack and predicts torsional critical speed frequencies at fixed non-integer ratios of lateral to torsional natural frequency. The spectrum of the torsional vibration is shown to contain super-synchronous critical speeds related to the lateral natural frequency. The unique frequency response of the torsional motion predicted by this model could be employed for early detection of a cracked rotor.

1. INTRODUCTION

The purpose of this investigation is to develop a model of cracked shaft vibration that identifies a distinct crack diagnostic measure observable with measured vibration data. This topic is widely studied because of possible sudden catastrophic failure of a rotor from fatigue. Stress concentrations and high rotational speeds exacerbate the problem. This is especially dangerous because the torsional response of the rotor is often unmeasured and because of low damping the torsional-lateral coupling may produce high amplitude torsional motion. A comprehensive literature survey of various crack modeling techniques and system behavior of cracked rotor was given by Wauer [1]. This paper contains the modeling of the cracked components of the structures and searches for different detection strategies to diagnose fracture damage. Dimarogonas [2] provided a comprehensive literature review of the vibration of cracked structures and cites more than 300 papers. The review is divided into several sections; methods that describe local flexibility due to cracks, nonlinearities introduced into the system, and local stiffness matrix descriptions of the cracked section. The crack leads to a coupled system that can be recognized from additional harmonics in the frequency spectrum. The sub-harmonic resonances at approximately half and one third of the bending critical speed of the rotor are reported to be the prominent crack indicators by Gash [3, 4] and Chan [5]. By utilizing a single parameter "hinge" crack model, Gasch, provided an overview of the dynamic behavior of a simple rotor with transverse crack. He assumed weight dominance and employed a perturbation method into his analysis. Cross-coupling stiffness and dynamic response terms were not included in his analysis. Mayes model [6] is more practical for deep cracks than a hinged model. Based on Mayes modified model, Sawicki and Wu et al. [7, 8] studied the transient vibration response of a cracked Jeffcott rotor under constant acceleration ratios and under constant external torque. The angle between the crack centerline and the rotor whirl vector is employed to determine the closing and opening of the crack. This allows one to study the rotor dynamic response with or without the rotor weight dominance assumption by taking non-synchronous whirl into account. Sawicki and Wu et al. [9] investigated the nonlinear dynamic response of a cracked one-mass Jeffcott rotor by means of bifurcation plots. When a rotor with the crack depth of 0.4 spins at some speed ranges, both the lateral and torsional vibration responses sustain periodic, quasi-periodic or chaotic behavior. Muszynska et al. [10] and Bently et al. [11] discuss rotor coupled lateral and torsional vibrations due to unbalance, as well as due to shaft anisotropy under a constant radial preload force. Their experimental results exhibited the existence of significant torsional vibrations due to coupling with the lateral modes. In Bently and Muszynska's experiments, an asymmetric shaft was used to simulate the behavior of a crack.

This paper extends the research investigations of both Bently et al. [11] and Wu's work [12]. While anisotropic shafts share some common characteristics with cracked shafts, the crack opening and closing introduces different behavior. Therefore, in this study an accurate and realistic crack model is introduced for a two-mass rotor in which the first mass represents a turbine and the second mass represents a generator. Starting from energy equations, an analytical model with four degrees of freedom for a torsional/lateral coupled rotor due to a crack is developed. A radial constant force is applied to the outboard disk to emphasize the effects of the gravity force which plays a critical role for the "breathing" of a crack. As preload increases, the vibration amplitudes in both lateral and torsional directions increase, making the measurements much easier to measure. The "second-order" nonlinear coupling terms due to a crack introduce super-synchronous peaks at certain rotational speeds, which is unique for a cracked rotor and might be used as an un-ambiguous crack indicator. Computer simulations also show that the rotational speeds at which amplitudes of the torsional vibrations reach maximum are governed by the ratio of lateral to torsional natural frequency.

2. EQUATIONS OF MOTION OF A CRACKED EXTENDED JEFFCOTT ROTOR

Figure 1 illustrates the system schematic configuration used to model a turbo machine with a cracked rotor. A Bently Nevada rotor kit of this configuration will be used in future experimental studies. The rotor is driven through a flexible coupling by an electric motor with a speed controller. A crack is located near the outboard disk. Shaft lateral vibrations are measured with a pair of proximity probes in horizontal and vertical orientations at the outboard disk where a downward constant radial force P is also applied. The coupled torsional-flexural vibrations are modeled using four degrees of freedom: torsional rotation at each disk and lateral motion at the outboard disk. Figure 2 show the section view of the cracked shaft, in both inertial (X, Y) and rotating coordinates (ξ, η).

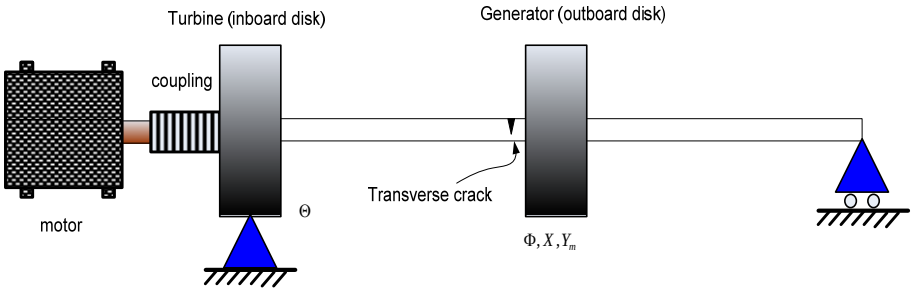

Figure 1. Configuration of the cracked extended Jeffcot rotor with two disks.

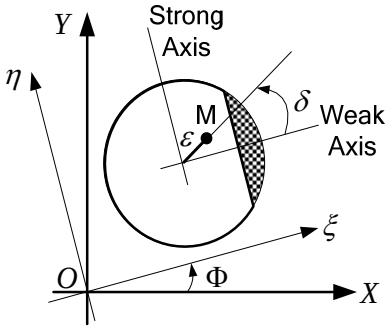

Figure 2. Section view of cracked shaft.

The angular position of the outboard disk is expressed as $\Phi(t)=\Omega t+\varphi(t)-\varphi_0$, where Ω is a rotational speed of the rotor, $\varphi(t)$ is a torsional angle of outboard disk relative to the motor, and φ_0 is the initial angular position. Similarly, the angular position of the inboard disk is expressed as $\Theta(t)=\Omega t+\theta(t)-\theta_0$, where $\theta(t)$ is the torsional angle of the inboard disk relative to the motor. The outboard disk's vibration is represented by the torsional coordinate $\Phi(t)$ and two lateral displacements in inertial coordinates. The inboard disk's vibration is described by the angle $\Theta(t)$. The location of the center of mass of the outboard disk can be expressed as the following:

$$\begin{aligned} x_{cm} &= X+\varepsilon\cos(\Phi+\delta) \\ y_{cm} &= Y+\varepsilon\sin(\Phi+\delta) \end{aligned} \tag{1}$$

The kinetic energy, potential energy and dissipation function for the cracked rotor system can respectively be expressed as the following:

$$\begin{aligned} T &= \frac{1}{2}I(\Omega+\dot{\varphi})^2+\frac{1}{2}I_0(\Omega+\dot{\theta})^2+\frac{M}{2}\left\{\dot{X}^2+\dot{Y}^2-2\varepsilon\dot{X}(\Omega+\dot{\varphi})\sin(\Phi+\delta)+2\varepsilon\dot{Y}(\Omega+\dot{\varphi})\cos(\Phi+\delta)+\varepsilon^2(\Omega+\dot{\varphi})^2\right\} \\ U &= \frac{1}{2}\left(k_{11}X^2+k_{22}Y^2\right)+k_{12}XY+\frac{1}{2}K_t(\varphi-\theta)^2 \\ D &= \frac{1}{2}C\dot{X}^2+\frac{1}{2}C\dot{Y}^2+\frac{1}{2}C_t(\dot{\theta}-\dot{\varphi})^2 \end{aligned} \tag{2}$$

The damping is modeled as lumped viscous damping at the outboard disk and lumped torsional viscous damping of the shaft. The stiffness matrix for a Jeffcott rotor with a cracked shaft in inertial coordinates, $\mathbf{K}_I$ is given [4,7,8] by the following. Details can be found in reference [12].

$$\mathbf{K}_I=\begin{pmatrix}k_{11} & k_{12}\\ k_{21} & k_{22}\end{pmatrix}=\begin{pmatrix}K & 0\\ 0 & K\end{pmatrix}-\frac{f(\Phi)K}{2}\begin{pmatrix}\Delta k_1+\Delta k_2\cos 2\Phi & \Delta k_2\sin 2\Phi\\ \Delta k_2\sin 2\Phi & \Delta k_1-\Delta k_2\cos 2\Phi\end{pmatrix} \tag{3}$$

$$\text{Where } \Delta k_1=\frac{\Delta k_\xi+\Delta k_\eta}{K} \text{ and } \Delta k_2=\frac{\Delta k_\xi-\Delta k_\eta}{K} \tag{4}$$

Δk_ξ, Δk_η are respectively the reduced stiffness in ξ and η directions in a rotor-fixed coordinate system. $f(\Phi)=\frac{1+\cos(\Phi)}{2}$ is a steering function which Mayes and Davies [6] proposed to illustrate a smooth transition

between the opening and closing of a “breathing” crack in rotating coordinates. $\Delta k_\eta = \Delta k_\xi / 6$ is assumed to describe the stiffness variation for deep cracks.

The general equations of motion are obtained using Lagrange’s equations.

$$\ddot{X} + \frac{C}{M}\dot{X} + \omega_n^2\left[1 - \frac{f(\Phi)}{2}\left(\Delta k_1 + \Delta k_2 \cos 2\Phi\right)\right]X - \frac{\omega_n^2 f(\Phi)\Delta k_2 \sin 2\Phi}{2}\left(Y_m - \frac{P}{K}\right)$$
$$= \varepsilon\left(\Omega + \dot{\varphi}\right)^2 \cos\left(\Phi + \delta\right) + \varepsilon\ddot{\varphi}\sin\left(\Phi + \delta\right)$$

$$\ddot{Y}_m + \frac{C}{M}\dot{Y}_m - \frac{\omega_n^2 f(\Phi)\Delta k_2 \sin 2\Phi}{2}X + \omega_n^2\left[1 - \frac{f(\Phi)}{2}\left(\Delta k_1 - \Delta k_2 \cos 2\Phi\right)\right]Y_m \tag{5}$$
$$= \varepsilon\left(\Omega + \dot{\varphi}\right)^2 \sin\left(\Phi + \delta\right) - \varepsilon\ddot{\varphi}\cos\left(\Phi + \delta\right) - \frac{Pf(\Phi)}{2M}\left(\Delta k_1 - \Delta k_2 \cos 2\Phi\right)$$

$$\ddot{\theta} + \frac{K_t + K_c}{I_0}\theta - \frac{K_t}{I_0}\varphi = -\frac{C_t + C_c}{I_0}\dot{\theta} + \frac{C_t}{I_0}\dot{\varphi}$$

$$\ddot{\varphi} + \frac{C_t}{I}\dot{\varphi} - \frac{C_t}{I}\dot{\theta} + \frac{K_t}{I}\varphi - \frac{K_t}{I}\theta = \frac{\mathrm{P}\,\varepsilon f(\Phi)}{2I}\left(\Delta k_1 \cos\left(\Phi + \delta\right) - \Delta k_2 \cos\left(\Phi - \delta\right)\right)$$
$$+ \frac{P^2}{2KI}\left[\frac{1}{2}\frac{\partial f(\Phi)}{\partial \Phi}\left(\Delta k_1 - \Delta k_2 \cos 2\Phi\right) + f(\Phi)\Delta k_2 \sin 2\Phi\right] + \Gamma_c$$

Where:

$$\Gamma_c = -\frac{C\varepsilon}{\rho^2 M}\left[\dot{X}\sin\left(\Phi + \delta\right) - \dot{Y}_m \cos\left(\Phi + \delta\right)\right] + \frac{\varepsilon\omega_n^2}{\rho^2}\left(1 - \frac{f(\Phi)}{2}\Delta k_1\right)\left[-X\sin\left(\Phi + \delta\right) + Y_m \cos\left(\Phi + \delta\right)\right]$$
$$+ \frac{\varepsilon f(\Phi)\Delta k_2 \omega_n^2}{2\rho^2}\left[-X\sin\left(\Phi - \delta\right) + Y_m \cos\left(\Phi - \delta\right)\right] + \frac{X^2\omega_n^2}{2\rho^2}\left[\frac{1}{2}\frac{\partial f(\Phi)}{\partial \Phi}\left(\Delta k_1 + \Delta k_2 \cos 2\Phi\right) - f(\Phi)\Delta k_2 \sin 2\Phi\right]$$
$$+ \frac{Y_m\left(Y_m - \frac{2P}{K}\right)\omega_n^2}{2\rho^2}\left[\frac{1}{2}\frac{\partial f(\Phi)}{\partial \Phi}\left(\Delta k_1 - \Delta k_2 \cos 2\Phi\right) + f(\Phi)\Delta k_2 \sin 2\Phi\right] \tag{6}$$
$$+ \frac{\Delta k_2 X\left(Y_m - \frac{P}{K}\right)\omega_n^2}{2\rho^2}\left[\frac{\partial f(\Phi)}{\partial \Phi}\sin 2\Phi + 2f(\Phi)\cos 2\Phi\right]$$

$Y = Y_m - \frac{P}{K}$ is used to delineate the static offset from dynamic response. Also, since $\varepsilon^2 \approx 0$, $I = I_0 + \varepsilon^2 M \approx I_0$ is assumed. Using non-dimensionalized time defined by the following:

$$\tau = \omega_n t,\ \ \frac{d(\cdot)}{dt} = \omega_n \frac{d(\cdot)}{d\tau} = \omega_n (\cdot)',\ \ \frac{d^2(\cdot)}{dt^2} = \omega_n^2 \frac{d^2(\cdot)}{d\tau^2} = \omega_n^2 (\cdot)'' \tag{7}$$

equations (5) and (6) take the following form:

$$X'' + 2\zeta X' + \left[1 - \frac{f(\Phi)}{2}\left(\Delta k_1 + \Delta k_2 \cos 2\Phi\right)\right]X - \frac{f(\Phi)\Delta k_2 \sin 2\Phi}{2}\left(Y_m - \frac{P}{M\omega_n^2}\right)$$
$$= \varepsilon\left(\frac{\Omega}{\omega_n} + \varphi'\right)^2 \cos\left(\Phi + \delta\right) + \varepsilon\varphi''\sin\left(\Phi + \delta\right)$$

$$Y_m'' + 2\zeta Y_m' - \frac{f(\Phi)\Delta k_2 \sin 2\Phi}{2} X + \left[1 - \frac{f(\Phi)}{2}\left(\Delta k_1 - \Delta k_2 \cos 2\Phi\right)\right] Y_m$$
$$= \varepsilon\left(\frac{\Omega}{\omega_n} + \varphi'\right)^2 \sin(\Phi + \delta) - \varepsilon\varphi'' \cos(\Phi + \delta) - \frac{P}{M}\frac{f(\Phi)}{2\omega_n^2}\left(\Delta k_1 - \Delta k_2 \cos 2\Phi\right) \tag{8}$$

$$\theta'' + (1 + K_r)\left(\frac{\omega_t}{\omega_n}\right)^2 \theta - \left(\frac{\omega_t}{\omega_n}\right)^2 \varphi = -2\zeta_t (1 + C_r)\frac{\omega_t}{\omega_n}\theta' + 2\zeta_t \frac{\omega_t}{\omega_n}\varphi'$$

$$\varphi'' + 2\zeta_t \frac{\omega_t}{\omega_n}\varphi' - 2\zeta \frac{\omega_t}{\omega_n}\theta' + \left(\frac{\omega_t}{\omega_n}\right)^2 \varphi - \left(\frac{\omega_t}{\omega_n}\right)^2 \theta = \frac{P}{2M}\frac{\varepsilon f(\Phi)}{\omega_n^2 \rho^2}\left(\Delta k_1 \cos(\Phi + \delta) - \Delta k_2 \cos(\Phi - \delta)\right)$$
$$+ \frac{P^2}{2M^2}\frac{1}{\omega_n^4 \rho^2}\left[\frac{1}{2}\frac{\partial f(\Phi)}{\partial \Phi}\left(\Delta k_1 - \Delta k_2 \cos 2\Phi\right) + f(\Phi)\Delta k_2 \sin 2\Phi\right] + \frac{\Gamma_c}{\omega_n^2}$$

$$\frac{\Gamma_c}{\omega_n^2} = -2\zeta \frac{\varepsilon}{\rho^2}\left[X' \sin(\Phi + \delta) - Y_m' \cos(\Phi + \delta)\right] + \frac{\varepsilon}{\rho^2}\left(1 - \frac{f(\Phi)}{2}\Delta k_1\right)\left[-X \sin(\Phi + \delta) + Y_m \cos(\Phi + \delta)\right]$$
$$+ \frac{\varepsilon f(\Phi)\Delta k_2}{2\rho^2}\left[-X \sin(\Phi - \delta) + Y_m \cos(\Phi - \delta)\right] + \frac{X^2}{2\rho^2}\left[\frac{1}{2}\frac{\partial f(\Phi)}{\partial \Phi}\left(\Delta k_1 + \Delta k_2 \cos 2\Phi\right) - f(\Phi)\Delta k_2 \sin 2\Phi\right]$$
$$+ \frac{Y_m\left(Y_m - \dfrac{2P}{M\omega_n^2}\right)}{2\rho^2}\left[\frac{1}{2}\frac{\partial f(\Phi)}{\partial \Phi}\left(\Delta k_1 - \Delta k_2 \cos 2\Phi\right) + f(\Phi)\Delta k_2 \sin 2\Phi\right]$$
$$+ \frac{\Delta k_2 X\left(Y_m - \dfrac{P}{M\omega_n^2}\right)}{2\rho^2}\left[\frac{\partial f(\Phi)}{\partial \Phi}\sin 2\Phi + 2 f(\Phi)\cos 2\Phi\right] \tag{9}$$

Where: $K_c = K_r K_t$, $C_c = C_r C_t$

Two special cases can be derived from the above general case.

Case 1 (pure torsional vibration)

Assuming no lateral vibration, $X = 0$, $Y_m = 0$, and a rigid drive coupling, $\dot{\Theta} = \Omega$, leads to the following simplification:

$$\ddot{\varphi} + \frac{C_t}{I}\dot{\varphi} + \frac{K_t}{I}\varphi = \frac{\mathrm{P}\,\varepsilon}{8I}\left(\Delta k_1 - \Delta k_2\right) + \left\{\frac{\mathrm{P}\,\varepsilon}{4I}\left(\Delta k_1 - \Delta k_2\right)\cos\Phi + \frac{P^2}{8KI}\left(-\Delta k_1 + \frac{\Delta k_2}{2}\right)\sin\Phi\right\}$$
$$+ \left\{\frac{\mathrm{P}\,\varepsilon}{8I}\left(\Delta k_1 - \Delta k_2\right)\cos 2\Phi + \frac{P^2 \Delta k_2}{4KI}\sin 2\Phi\right\} + \frac{3P^2 \Delta k_2}{16KI}\sin 3\Phi \tag{10}$$

Introducing the following two constants:

$$E_1 = \frac{\mathrm{P}\,\varepsilon}{2I\omega_n^2} = \frac{P}{2M}\frac{\varepsilon}{\rho^2\omega_n^2},\quad E_2 = \frac{\mathrm{P}^2}{2KI\omega_n^2} = \frac{P^2}{2M^2}\frac{1}{\rho^2\omega_n^4} \tag{11}$$

The non-dimensional form of equation (10) becomes:

$$\varphi'' + 2\zeta_t \frac{\omega_t}{\omega_n}\varphi' + \left(\frac{\omega_t}{\omega_n}\right)^2 \varphi = \frac{E_1}{4}\left(\Delta k_1 - \Delta k_2\right) + \left\{\frac{E_1}{2}\left(\Delta k_1 - \Delta k_2\right)\cos\Phi + \frac{E_2}{4}\left(-\Delta k_1 + \frac{\Delta k_2}{2}\right)\sin\Phi\right\}$$
$$+\left\{\frac{E_1}{4}\left(\Delta k_1 - \Delta k_2\right)\cos 2\Phi + \frac{E_2\Delta k_2}{2}\sin 2\Phi\right\} + \frac{3E_2\Delta k_2}{8}\sin 3\Phi \qquad (12)$$

Case 2 (lateral vibration without torsional vibration)

In this case the cracked rotor is considered as laterally flexible and torsionally rigid. Therefore, the system could be described by the first two equations of (5) in which φ and θ are assumed zero. Since similar scenarios are well studied in [4,5,7,12], it is not explored here except to note that the general model presented in this work reduces to known models under these assumptions.

$$\ddot{X} + \frac{C}{M}\dot{X} + \omega_n^2\left[1 - \frac{f(\Omega t)}{2}\left(\Delta k_1 + \Delta k_2\cos(2\Omega t)\right)\right]X - \frac{\omega_n^2 f(\Omega t)\Delta k_2 \sin(2\Omega t)}{2}\left(Y_m - \frac{P}{K}\right)$$
$$= \varepsilon\Omega^2\cos(\Omega t + \delta)$$
$$\ddot{Y}_m + \frac{C}{M}\dot{Y}_m - \frac{\omega_n^2 f(\Omega t)\Delta k_2 \sin(2\Omega t)}{2}X + \omega_n^2\left[1 - \frac{f(\Omega t)}{2}\left(\Delta k_1 - \Delta k_2\cos(2\Omega t)\right)\right]Y_m$$
$$= \varepsilon\Omega^2\sin(\Omega t + \delta) - \frac{Pf(\Omega t)}{2M}\left(\Delta k_1 - \Delta k_2\cos(2\Omega t)\right) \qquad (13)$$

3. RESULTS AND DISCUSSION

Computer simulation results using the parameters in table 1 for the case of pure torsion without lateral vibration are illustrated in figure 3. This response which is calculated using equation 10 can be interpreted as a nonlinear oscillator with 1X excitation $\left\{\frac{\mathrm{P}\,\varepsilon}{4I}\left(\Delta k_1 - \Delta k_2\right)\cos\Phi + \frac{P^2}{8KI}\left(-\Delta k_1 + \frac{\Delta k_2}{2}\right)\sin\Phi\right\}$, 2X excitation $\left\{\frac{\mathrm{P}\,\varepsilon}{8I}\left(\Delta k_1 - \Delta k_2\right)\cos 2\Phi + \frac{P^2\Delta k_2}{4KI}\sin 2\Phi\right\}$, and a 3X excitation $\left\{\frac{3P^2\Delta k_2}{16KI}\sin 3\Phi\right\}$ due to the unbalance, the depth of the crack and the side load.

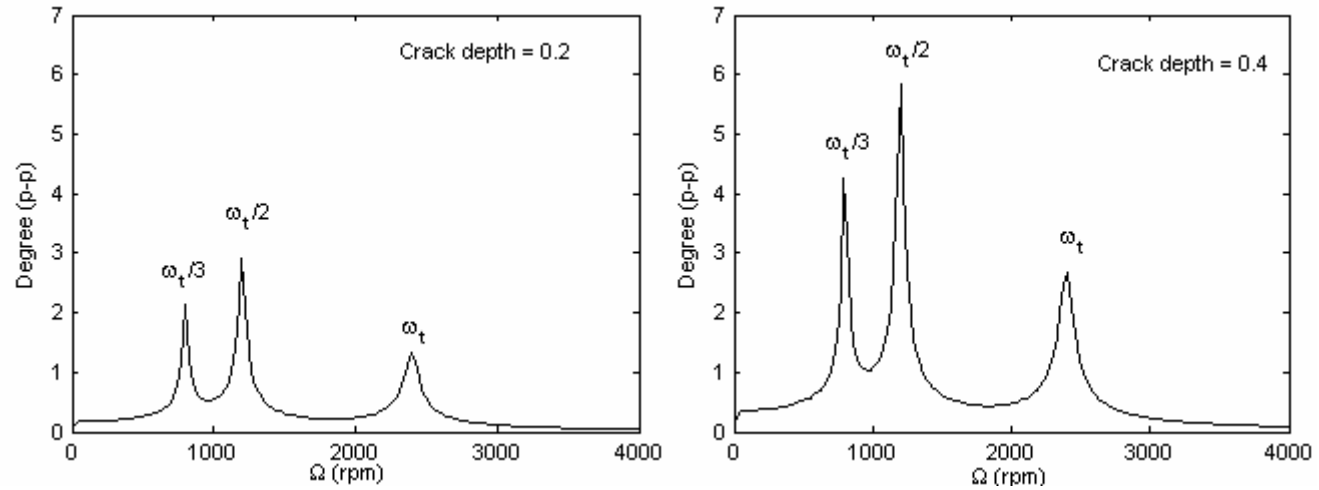

(a). $\Delta k_\xi / K$ = 0.2 (b). $\Delta k_\xi / K$ = 0.4

Figure 3. Peak-to-peak torsional vibration response, φ, from case 1.

In addition to the excitations noted above, the constant forcing excitation $\frac{P\varepsilon}{8I}(\Delta k_1 - \Delta k_2)$ is also present. It is worthy to notice that the crack depths Δk_ξ, Δk_η, contained in $\Delta k_1, \Delta k_2$ which are originally introduced from the lateral stiffness terms, significantly affect the torsional vibration amplitude. Note that these vibrations would require torsional transducers for measurement.

When the parameters shown in table 2 are used in the general four degree of freedom model, the critical frequencies shift from those shown above (see figure 4). Critical speeds are no longer at integer fractional multiples of the torsional natural frequencies. Instead, for a given ratio of torsional to lateral natural frequency critical speeds occur at fixed non-integer multiples of the lateral natural frequency. When the frequency ratio is changed the critical speeds shift.

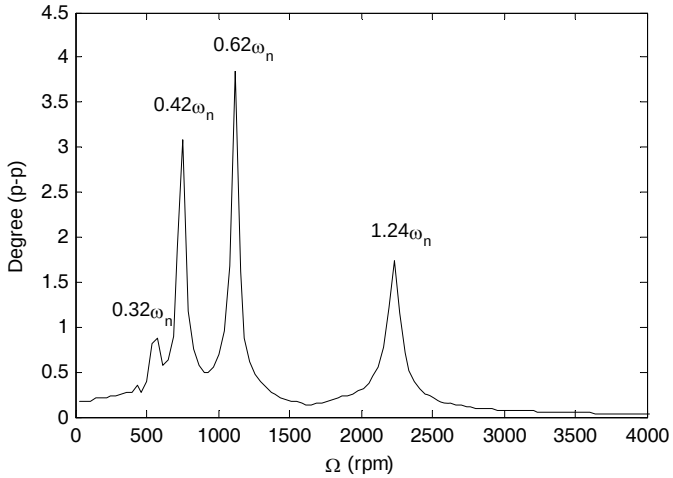

(a). ω_t / ω_n = 1.38; ω_n =1800 rpm

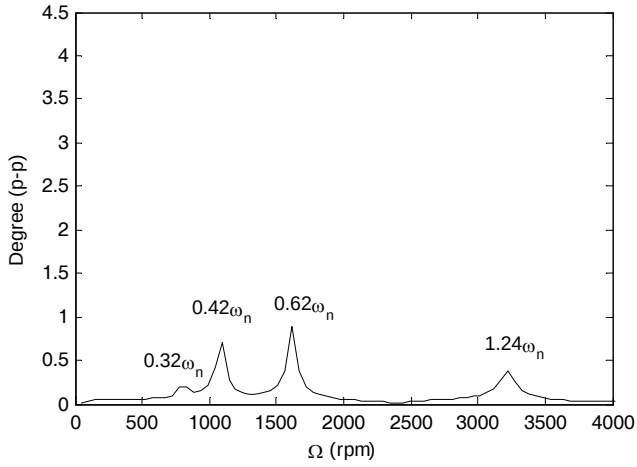

(b). ω_t / ω_n = 1.38; ω_n =2600 rpm

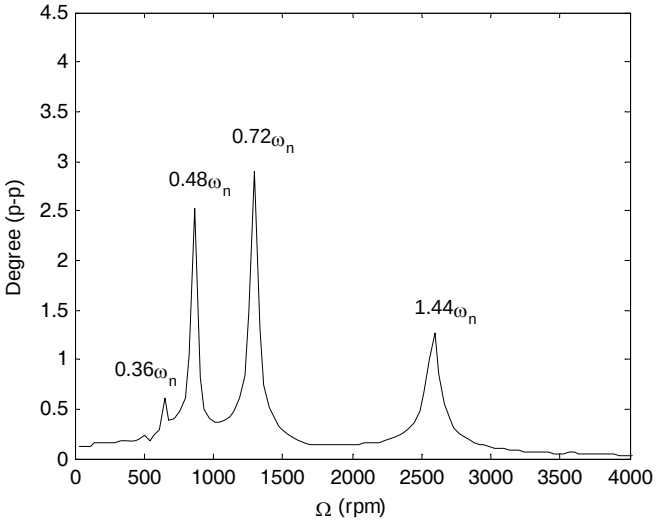

(c). ω_t / ω_n = 1.6; ω_n =1800 rpm

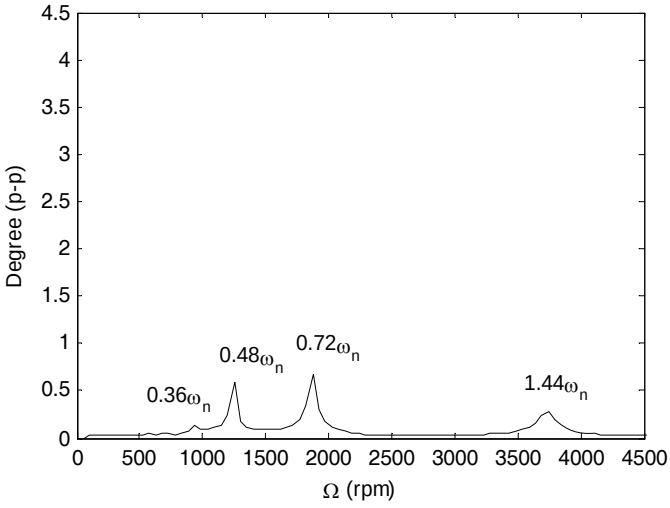

(d). ω_t / ω_n = 1.6; ω_n =2600 rpm

Figure 4. Peak-to-peak torsional vibration response φ from general lateral/torsional coupling case.

The steady state response at one third the lateral natural using the same parameters as in (d) above is shown in figure 5. The orbit has three loops from the 3x excitation. The x-probe shows significant super-synchronous response. The spectrum of the torsional vibration contains super-synchronous critical speeds related to the lateral natural frequency.

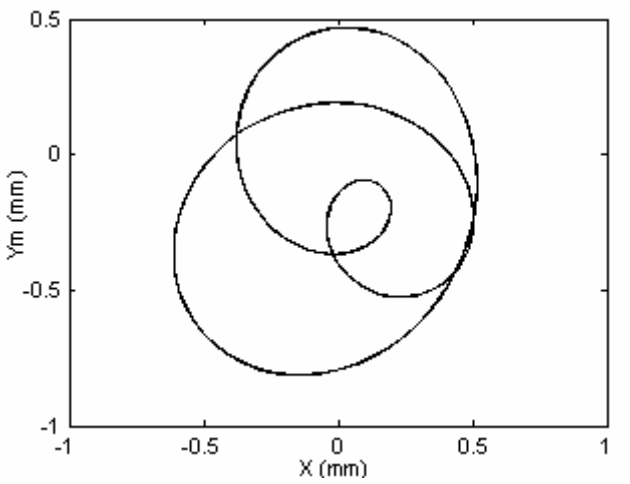

(a). Orbit

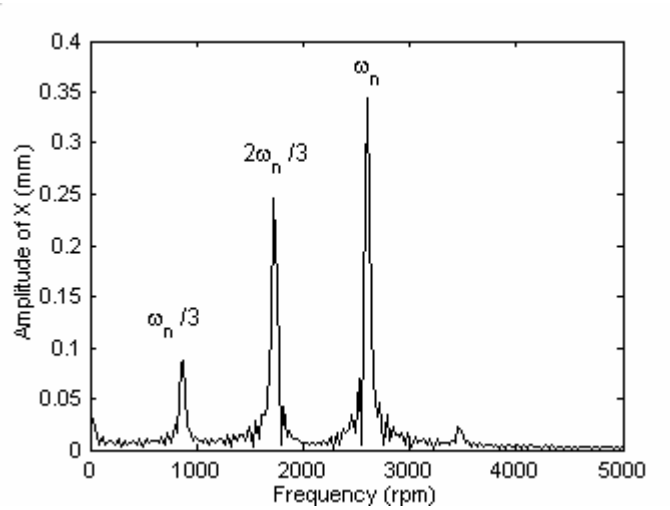

(b). FFT of X

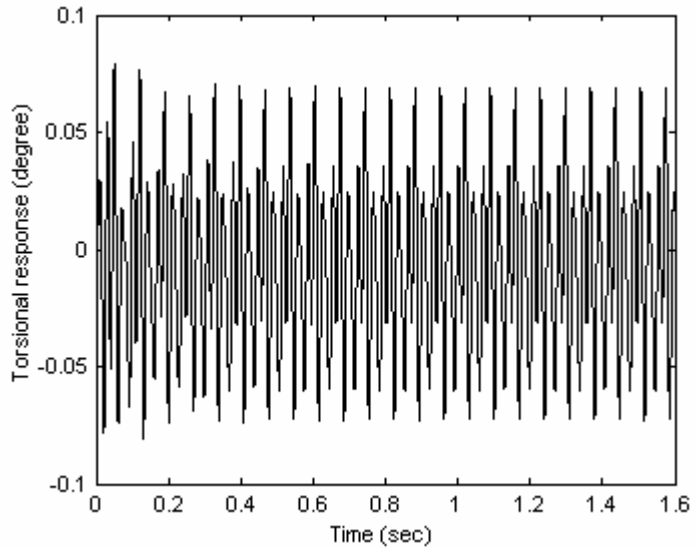

(c).Torsional response

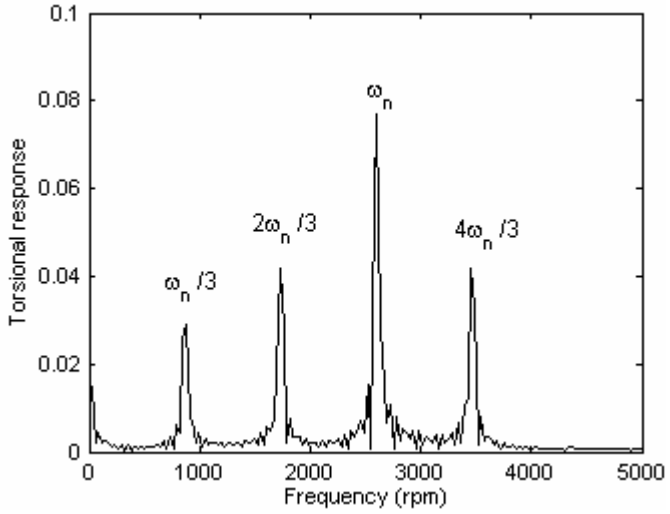

(d). FFT of φ

Figure 5. The vibration responses at $\Omega = \omega_n/3$; ω_t / ω_n = 1.38; ω_n =2600 rpm.

Table 1: Model Physical Parameters for Pure Torsional Vibration, Case 1

Parameters	Value	Units
ω_n	10800	rpm
ω_t	2400	rpm
ε	15.24×10^{-5}	m
ρ	0.02286	m
P/M	1016	m/s^2
ζ_t	0.02	

Table 2: Model Physical Parameters for Torsional and Lateral Vibration, General Case

Parameters	Value	Units
ε	5.08×10^{-5}	m
ρ	0.02286	m
P/M	101.6	m/s^2
ζ_t	0.02	
ζ	0.1	
K_r	5	
C_r	1	
$\Delta k_{\xi} / K$	0.38	

4. CONCLUSIONS

This paper documents the effect of a shaft crack on lateral and torsional vibrations of a two-mass rotor system. An analytical model of an extended Jeffcott rotor is first derived from Lagrange's equations taking into consideration lateral/torsional vibration coupling mechanism induced by a "breathing" of a crack. The vibration behavior of a large class of machines such as turbine-generator sets or other machines with two primary rotary inertias can be described by this simplified equivalent configuration. Four degrees of freedom describe the model: two lateral displacements and one torsional angular displacement of an outboard disk, and the torsional angular displacement of an inboard disk. The nonlinearities associated with a breathing crack couple the four equations of motion. Two cases are considered in this work; a torsionally rigid rotor without lateral vibration and a general unconstrained solution to the four degree of freedom model presented. The first case illustrates substantial vibrations, which could be easily captured by the torsional transducers, happen at $\Omega = \omega_t / 3$ and $\Omega = \omega_t / 2$. With an increase in crack depth, the resonance peaks at 1×, 2× and 3× of the torsional vibration increase dramatically. The general case makes evident the existence of strong coupling between lateral and torsional vibrations due to the crack and side load. Nonlinear lateral-torsional coupling from a crack shifts the fundamental resonance peak in the torsional vibration response. The resonance peak frequencies shift depending on the ratio of the lateral to torsional natural frequencies with the peak responses occurring at fixed non-integer values of the lateral natural frequency for any particular frequency ratio. Whereas, the amplitudes will vary according to crack depth, loading, and relative stiffness. The lateral orbit and torsional steady-state time response, induced by the interaction between transverse crack and side load, are also portrayed. The distinct vibration signatures predicted by this model can be used for shaft crack diagnostic purposes. Based on the numerical simulation results, experimental tests will be designed in future investigations.

ACKNOWLEDGEMENTS

This work was sponsored by the Department of the Navy, Office of Naval Research, under Award # N00014-05-1-0855. This support is gratefully acknowledged. The authors also wish to acknowledge the support of the Donald E. Bently Center for Engineering Innovation at California Polytechnic State University San Luis Obispo for support of this work.

REFERENCES

[1]. Wauer, J., 1990, “On the Dynamics of Cracked Rotors: A Literature Survey”, *Applied Mechanics Reviews*, Vol. 43(1), pp. 13-17.

[2]. Dimarogonas, A. D., 1996, “Vibration of Cracked Structures: A State of the Art Review,” *Engineering Fracture Mechanics*, Vol. 55 (5), pp. 831 – 857.

[3]. Gasch, R., 1976, “Dynamic behavior of a simple rotor with a cross-sectional crack”, *Paper C178/76, I. Mech. E. Conference on Vibrations in Rotating Machinery*, pp.123-128.

[4]. Gasch, R. A, 1993, “Survey of the Dynamic Behavior of a Simple Rotating Shaft with a Transverse Crack”, *Journal of Sound and Vibration* Vol. 162, pp313-332.

[5]. Chan, R. K. C. and Lai, T. C., 1995, “Digital Simulation of a rotating shaft with a transverse Crack,” *Appl. Math. Modelling* Vol. 19, July pp. 411-420.

[6]. Mayes, I. W. and Davies, W. G. R., 1984, “Analysis of the Response of a Multi-Rotor-Bearing System Containing a Transverse Crack in a Rotor”, *ASME Journal of Vibration, Acoustics, Stress, and Reliability in Design*, Vol. 106, pp 139-145.

[7]. Sawicki, J. T., Wu, X., Baaklini, G.Y. and Gyekenyesi, A., 2003, “Vibration-Based Crack Diagnosis in Rotating Shafts During Acceleration Through Resonance”, *Proceedings of SPIE*, Vol. 5046.

[8]. Sawicki, J. T., Bently, D. E., Wu, X., Baaklini, G.Y. and Friswell, M. I., 2003, “Dynamic Behavior of Cracked Flexible Rotor Subjected to Constant Driving Torque”, ISCORMA-2, Gdańsk, Poland, 4-8, August 2003, pp. 231-241.

[9]. Sawicki, J.T., Wu, X., Gyekenyesi, A. L. and Baaklini, G. Y., 2005 “Application of Nonlinear Dynamic Analysis for Diagnosis of Cracked Rotor Vibration Signatures”, submitted to SPIE International Symposium, San Diego, California USA, March 7-10.

[10]. Muszynska, A., Goldman, P. and Bently, D. E., 1992, “Torsional/Lateral Cross-Coupled Responses Due to Shaft Anisotropy: A New Tool in Shaft Crack Detection”, *I. Mech. E., C432-090, Bath, United Kingdom*, pp. 257-262.

[11]. Bently, D. E., Goldman, P. and Muszynska, A., 1997, ““Snapping” Torsional Response of an Anisotropic Radially Loaded Rotor,” *Journal of Engineering for Gas Turbines and Power*, Vol. 119, pp. 397-403.

[12]. Wu, X., 2005, Doctoral dissertation, “Vibration-based Crack-induced Damage Detection of Shaft-disk System”, Cleveland State University.